

Thermodynamic Considerations in the Application of Reverse Mode Gasification to the Destruction of Hazardous Substances

DAVID W. LARSEN* AND
MICHAEL D. WASHINGTON

Department of Chemistry, University of Missouri—St. Louis,
St. Louis, Missouri 63121

STANLEY E. MANAHAN AND
BRADLEY MEDCALF

Department of Chemistry, University of Missouri—Columbia,
Columbia, Missouri 65211

FRANK E. STARY

Department of Chemistry, Maryville University,
St. Louis, Missouri 63141

Previous studies by us have demonstrated the effectiveness of reverse mode gasification using a granular char matrix for treatment of hazardous wastes. Calculations pertaining to this gasification are presented, including a one-dimensional temperature profile and a thermodynamic analysis. Equilibrium compositions were calculated by free energy minimization using commercially available software. The calculated results were compared with experimental data for gasification of mixtures containing water, selected hydrocarbons, and used motor oil. Batch and continuous feed reactors were used with optimized operating parameters to generate the data. The dry gas product obtained from gasification of water and selected hydrocarbons contains carbon dioxide, carbon monoxide, methane, and hydrogen, in agreement with thermodynamic predictions, and the compositions agree well with predictions obtained assuming that chemical equilibrium is attained at a temperature of 650 °C. The dry gas product from gasification of motor oil contains small amounts of low molecular weight hydrocarbons, which are not thermodynamically stable, but the composition of the major products generally agrees with the thermodynamic predictions. Under optimized conditions, the aqueous condensate contains between 1 and 100 ppm organics. Heat balance terms for the process were also calculated, and these demonstrate the efficiency of gasification as a treatment method.

Introduction

We have shown (1–12) that “reverse mode” (13) gasification which uses a specially prepared char support matrix is convenient and effective in treating a variety of hazardous substances. Reverse mode gasification as a continuous process can be run using the configuration shown in Figure

1. A granular subbituminous coal char with a macroporous surface is used to sorb the waste. If required, water is added to facilitate gasification. The details for preparing the char and its sorption properties have been presented elsewhere (2, 4–8). After sorbing the waste, the char remains a dry granular solid, easy to handle, so that problem materials such as oily sludges can be readily processed. The char/waste mixture is charged to the feed hopper and subsequently into the cylindrical reactor. The granular char serves as a gas permeable support matrix for the process. Heat is applied at the ignition point, and O₂ gas is fed in at the top of the reactor. After a short time, an incandescent thermal zone (ITZ) forms spontaneously at the point of heating, at which time heating is no longer required.

The ITZ is a narrow, high-temperature zone, typically less than 1 cm high, but spread evenly across the entire cross-section of the reactor. In batch mode gasification, the ITZ passes upward, once through the entire length of the char bed, against the gas flow. In continuous operation, as shown, the upward ITZ movement is balanced by the downward movement of the char bed, as controlled by the valve, so that the ITZ remains stationary within the reactor. Within the ITZ, oxidative chemistry occurs with release of a large amount of heat, giving rise to localized temperatures up to an estimated 2000 °C. Visually the zone appears “white hot”. Reactions occur on the surface of the char and in the gas phase. The heat of reaction is supplied primarily by the oxidation of organics in the waste, and little of the char is consumed. The region immediately above the ITZ is at ambient temperature. Immediately below the ITZ, the temperature is about 900 °C, and the char has a dull red appearance. At the bottom edge of the ITZ and below, oxygen is depleted so that the hot bed is both highly reactive and chemically reductive. This facilitates reductive endothermic chemistry and formation of the combustible gas mixture that is characteristic of gasification. The endothermic processes and heat loss cause continued cooling of the bed, and the temperature decreases in the vertical direction to about 500 °C at the bottom of the reactor.

The product gas leaving the bottom of the reactor passes through a condenser, from which the dried gas emerges clean-burning, with a moderate fuel value (e.g., 300 Btu/(standard ft³)). The overall result is that the organic and aqueous portions of the waste are removed from the char, with only a small amount (e.g., 10%) of char consumption. The recovered char is thus regenerated and can be recycled. It also serves as a trap for undesirable byproducts.

Temperature Profile. A one-dimensional theoretical analysis of the complex temperature profile for underground coal gasification derived from the heat equation has been presented (14). The treatment is generally applicable to the gasification studies described herein. Heat balance on the element includes terms for heat transfer (by convection, conduction, and heat loss), mass transfer (flow of gases), chemical reaction kinetics, and reaction enthalpies. A single Arrhenius equation for the rate and separate reaction enthalpies for the exothermic and endothermic processes were used for simplicity. The resulting differential equations require numerical solution. The predicted temperature profile using parameters applicable to underground coal gasification (14) is shown in Figure 2. The temperature profile represents a front that moves along the bed (or reactor) axis at a fixed velocity, depending on the values of the operating parameters; movement is from right to left in the figure. The ITZ is at the temperature maximum, denoted by the dashed line. The coal (or untreated feedstock) resides at the left, in the region

* Phone: (314) 516-5341; fax: (314) 516-5342; e-mail: larsen@jinx.umsl.edu.

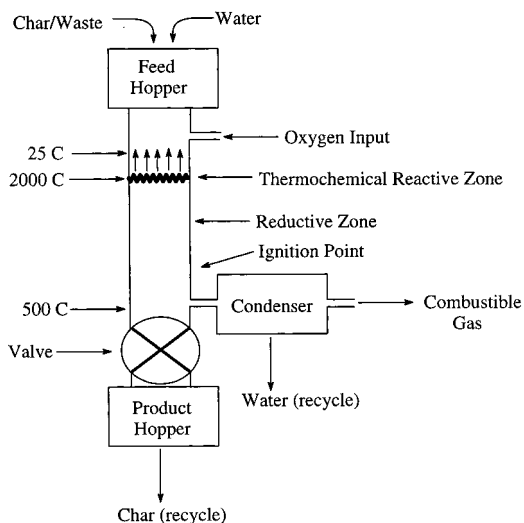


FIGURE 1. Schematic of apparatus used for continuous feed reverse mode gasification.

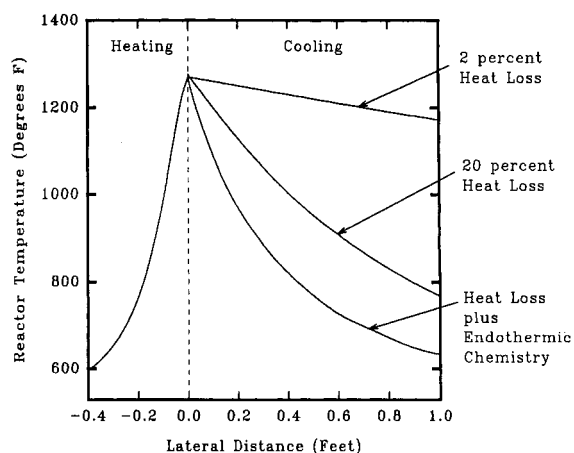


FIGURE 2. Temperature profile for reverse mode gasification. The one-dimensional model represents a thermal front that passes through a porous carbonaceous bed (see text for further details). The parameters used to generate the plot are appropriate for underground coal gasification.

marked "heating", where the temperature increases rapidly and exponentially as the ITZ moves. Movement is caused by conduction of heat into the oxygen-rich region ahead (left) of the ITZ, which causes the reaction rate to increase with increasing temperature until the oxygen is completely depleted at the point of maximum temperature. Gasified char resides at the right, in the oxygen-depleted region marked "cooling," where the temperature falls off more gradually with movement of the ITZ. In the original treatment (14) the rate of thermal decay in this region was attributed solely to heat loss. We have modified the equations to also include the effects of endothermic chemistry, which also contribute to cooling, as shown. Quantitatively, Figure 2 applies strictly to coal gasification, but the qualitative features are the same as those in the present studies, so the figure is of use in visualizing the gasification process. The quantitative differences are attributable to the present use of oxygen, as opposed to air in coal gasification, to the neglect of radiative heat transfer (which is not as important in coal gasification with air but which should be important in the present studies) and to the differences between waste laden char and coal.

The one-dimensional gasification model, even though oversimplified, is still complex.

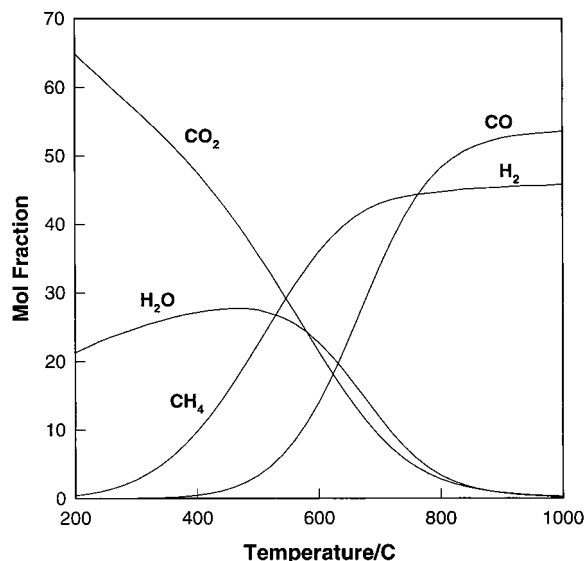


FIGURE 3. Calculated composition of product gas in reverse mode gasification. The composition depends strongly on the thermal equilibrium temperature as shown.

Thermodynamics provides the driving force, but kinetic factors may control the chemistry, especially since the residence time within the ITZ is relatively short. A thermodynamic analysis of the process is given below. In addition, studies to optimize process parameters are described.

Finally, as a first attempt to determine whether kinetic limitations exist, the observed composition of the gas product is compared with the predicted equilibrium composition.

Thermodynamic Analysis. An important thermodynamic consideration in gasification of organics and water on char is the temperature-dependent equilibrium distribution of products. This can be calculated with readily available computer software (15). To illustrate, consider a simple model system comprised of a char containing octane (representing the organic content of a waste) and water which is gasified using oxygen. The composition, which is typical for reverse mode gasification, is 1 mol of $C_8H_{18}(l)$, 38.5 mol of $C(s)$, 6.4 mol of $H_2O(l)$, and 5.8 mol of $O_2(g)$. This is a heavily loaded char, organics and water each being 25% of the char weight. The char is assumed to be graphite, denoted as $C(s)$ (16), and any of the large number of compounds in the database can be included in the computation. After the starting composition is specified, the equilibrium composition of this system can be calculated at any desired temperature and pressure. Thermodynamic data from the database (17) are used, and the total free energy of the system is minimized (18). The results are shown in Figure 3, where the gas-phase product distribution is plotted as a function of temperature, at 1 bar pressure. It can be seen that the results are very simple; there are only five thermodynamically stable product gases. The composition is temperature-dependent; CH_4 , CO_2 , and H_2O are predominant at low temperatures, and the high-temperature products are CO and H_2 . The ratio of the products depends on the starting composition of the system, but the same gases and the same qualitative trends are always predicted regardless of the hydrocarbon present initially. Oxygen-containing organics are also converted to these five gases. Of special interest, it can be seen that if water is removed with a condenser, the remaining gases should have a moderately high Btu content at temperatures above about 600 °C.

$C(s)$, not shown in the figure, is also present in large excess across the entire temperature range. At low temperatures, near 200 °C, additional C is formed (about 10% excess). $C(s)$ gradually decreases as the temperature increases; about 5%

is consumed in the intermediate temperature range, near 600 °C. In the high-temperature range, C(s) decreases further so that about 25% is consumed at 800 °C, and above this temperature, no further C is consumed.

If the results shown in Figure 3 are extended to higher temperature, radicals are predicted; e.g., at 2000 °C, the estimated temperature within the ITZ, one obtains 0.02 mol H, 10^{-3} mol CH₃, and 10^{-6} mol OH. The efficient destruction of refractory organics, e.g., chlorinated compounds, has been attributed especially to the presence of H (8).

The fate of heteroatoms can be similarly determined. Two common ones of interest are S and N because of the potential formation of SO_x and NO_x. This problem does not occur with reverse mode gasification as described herein. The stable sulfur-containing species predicted during gasification are S, COS, and H₂S (19), and the stable nitrogen-containing species are N₂, HCN, and NH₃ (11).

From Figure 3, the equilibrium product composition at a given temperature and 1 bar can be determined. In general, these data illustrate the thermodynamic driving force for the process. However, they also allow quantitative predictions to be made if one assumes that the system comes to equilibrium at some temperature. The results of our previous studies generally support this approach. First, the gas product is combustible, and within certain ranges of operating parameters, it is possible to get a clean-burning gas product, i.e., one that burns with a blue flame. This indicates that larger molecular weight hydrocarbons are present only at low levels. The gas composition suggests that the temperature for equilibrium is between 600 and 700 °C. The limits of combustibility of gases in air (20) are as follows: hydrogen, 4–74%; methane, 5–15%; carbon monoxide, 12.5–74.2%. Inspection of Figure 3 shows that, for temperatures above about 400 °C, the equilibrium gas product mixture should sustain combustion. Second, water is present in the gas product, and it is conveniently condensed and recycled in the process. This indicates an equilibrium temperature below 800 °C. Third, char loss during gasification is typically 10% or less, which also suggests an equilibrium temperature below about 700 °C. Temperatures within the ITZ are markedly higher than these values; in fact to ascribe a temperature to the ITZ is an oversimplification since exothermic gas-phase reactions are the primary source of heat, and the heat must then flow to the interior of the char particles. Direct measurements with high-temperature thermocouples inserted in the ITZ have yielded readings of 1400 °C, but actual gas-phase temperatures are probably higher; we estimate 2000 °C. Endothermic processes in the reduction zone cause the temperature to fall rapidly as the gas moves through the reactor so that the gas normally exits the reactor at about 500 °C. The magnitude of these temperatures indicates that establishment of equilibrium must occur in the reductive zone. Last, SO_x and NO_x in the gas product are generally unobservable, also in accord with the thermodynamic predictions.

The quantitative application of these data to gasification is not obvious because of the complex temperature profile and also because the kinetics of the chemical reactions are undoubtedly complex. However, the equilibrium predictions can be considered with the following rationale. First, the temperature decreases rapidly as the gases leave the ITZ and pass through the reductive or cooling zone. Second, the rates of reaction are highly temperature-dependent, and these will decrease markedly along the axis of the reactor. Thus, we consider that, at some position, there is a cutoff temperature, below which the reaction rates are negligible so that equilibrium is established at that temperature. As a test of this approach, experimental gas compositions can be compared with the thermodynamic predictions to determine whether agreement can be found at some temperature.

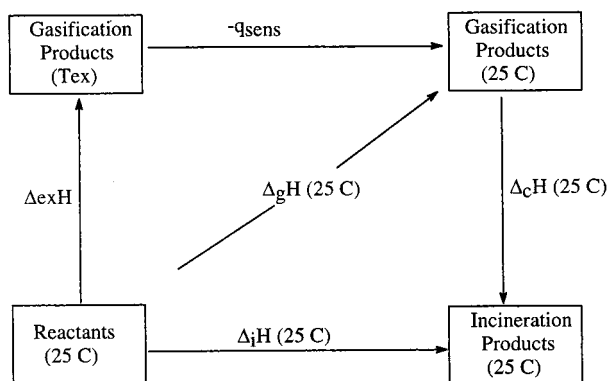


FIGURE 4. Diagram illustrating thermodynamic heat balance terms in reverse mode gasification.

A second important thermodynamic consideration is heat balance in gasification. This can be discussed in terms of the process diagram shown in Figure 4. Gasification per se as it occurs within the reactor is described by the vertical process on the left, where T_{ex} is the exit temperature of the gas product and $\Delta_{ex}H$ is the reaction enthalpy, which is the heat lost to the surroundings during the process. Under adiabatic conditions, i.e., when $\Delta_{ex}H = 0$, T_{ex} equals T_a , the adiabatic temperature, which is the highest temperature attainable at the exit port of the reactor. The sensible heat, $-q_{sens}$, is that which must be removed from gas and char products to reduce the temperature from T_{ex} to 25 °C. $\Delta_gH(25\text{ °C})$ refers to gasification in the standard state. Finally, burning the gas mixture releases the (standard state) heat of combustion, $\Delta_cH(25\text{ °C})$. Idealized incineration produces complete combustion products (CO₂ and H₂O) with corresponding standard state $\Delta_iH(25\text{ °C})$. The unique features of gasification in contrast to incineration can be demonstrated numerically with reference to Figure 4.

Before determining the adiabatic temperature, it is useful to consider the gas-phase reactions per se. These strongly exothermic processes lead to very high temperatures in the gas phase, which would be characterized in the limit of no vapor-phase heat loss, by an adiabatic flame temperature (21), which is typically >2000 °C. This high temperature is consistent with the observed ITZ and the presence of radicals as discussed above. However, we will consider the adiabatic temperature to be that in which heat is allowed to flow to the char. Since char is present in large excess, the resulting adiabatic temperature will be lower than the adiabatic flame temperature.

T_a for the model system described above was found with the use of the thermodynamics software (22) to be 714 °C. This value serves as a check on the calculation because it must be above the observed exit temperature, which is about 500 °C. Next, we consider a nonadiabatic gasification. It is necessary to specify an equilibrium temperature for the products, which will determine the composition. We will show below that a reasonable value for the equilibrium temperature is 650 °C. A typical experimental exit temperature, T_{ex} is 500 °C. The calculated enthalpy values for heat balance in gasification are then

$\Delta_{ex}H$	$-q_{sens}$	$\Delta_gH(25\text{ °C})$	$\Delta_cH(25\text{ °C})$	$\Delta_iH(25\text{ °C})$
-819 kJ	-647 kJ	-1466 kJ	-5321 kJ	-6787 kJ

$\Delta_{ex}H$, the heat lost to the surroundings during gasification, is about 12% of Δ_iH . The sensible heat q_{sens} , which is that contained by the products by virtue of these being at elevated temperature, is about 10% of Δ_iH . Both these quantities can be partially recovered with heat exchangers. An important

measure of the efficiency of the process is $\Delta_c H / \Delta_i H$, the ratio of the heat released in the combustion of gas products to that of incineration. In the present case the ratio is 78%, and this illustrates very clearly how resource recovery, in the form of fuel gas, can be produced along with destruction of hazardous materials.

The thermodynamic basis for reverse mode gasification is thus established. However, the analysis is subject to kinetic limitations. We note that when this method is used for the treatment of hazardous mixtures, the aqueous condensate and char product can be conveniently recycled. This is fortunate because both char and condensate serve to trap hazardous substances while allowing synthesis gases to emerge. In practice a char filter may also be placed at the outlet of the condenser, and this char can also be regenerated in the process. The most important requirement is that the product gas be free from hazardous byproducts. In the remainder of this report, we present results of several studies to determine the extent to which equilibrium compositions can actually be obtained in reverse mode gasification. We also present thermodynamic analyses of the experimental results, which broaden our understanding of the process.

Experimental Section

Reactors. Batch mode gasifications were conducted in a 1 in. diameter by 1 ft length Vycor tube and in stainless steel tubes (1 and 1.75 in. diameter) by 2.5 ft. Continuous feed gasifications were conducted with a 2 in. diameter stainless steel reactor (as described in Figure 1).

Char. One type of char used in the studies was prepared by gasifying coal multiple times in reverse mode. A second type of char was prepared by pyrolyzing coal.

Gas Sampling. Effluent from reactors passed through a cold trap set in an ice bath, which served to remove condensables. The trap was fitted with a sidearm for the collection of the off gases. The gas samples were then collected in 2 L Tedlar gas sample bags and immediately analyzed to prevent reactions from occurring that might significantly alter the gas composition.

Condensates. Condensates were extracted with 3 mL of deuterated chloroform prior to GC/MS or NMR analysis.

Gas Chromatography. Samples were analyzed for H_2 , CO, CH_4 , and CO_2 , using a Shimadzu Model GC-14A gas chromatograph with a carboxsphere 80/100 column (Alltech, 6 ft \times 1/8 in.), a thermal conductivity detector, and an air-actuated 1 mL gas sample loop. The oven temperature program was 35 °C for 2 min and ramped at 20 °C/min to 155 °C. The detector temperature and current were set to 155 °C and 125 mV, respectively. Helium was used as a carrier gas with a flow rate of 25.00 mL/min and a makeup flow of 20 mL/min. Gases were identified by comparing retention times with standards of the pure gases. Calibration curves were produced using the pure gas standards.

GC/MS. Measurements were made using a Hewlett-Packard GC 5890 Series II gas chromatograph with a Hewlett-Packard MS quadrupole engine MS 59827A. The GC was equipped with a 0.32 mm i.d. \times 30 m DB-5 column operated at 50 °C for 4 min and then ramped 8 °C/min to 300 °C. The mass spectrometer scan covered the range from 50 to 800 Da. The Wiley/NBS Registry of MS Spectral Data Library was used for compound identifications.

High-Resolution Nuclear Magnetic Resonance. Nuclear magnetic resonance (NMR) spectra were obtained with either a 300 or 400 MHz Varian NMR spectrometer containing a four-nucleus NMR probe (5 mm) for observing 1H , ^{19}F , ^{13}C , and ^{31}P .

Results and Discussion

Gasification of Char Containing Water. Dry char is not a

good medium for gasification. The simplest system for gasification is char containing a small amount of water. Thus, as a starting point, we consider char containing 10% water based on char weight. Gasification of this system does not require optimization since it is relatively insensitive to oxidant flow. Because of its simplicity, this should be the ideal system with which to compare the experimental and calculated gas compositions. Reverse mode gasification with a Vycor reactor using oxygen gave the following dry gas product with composition, as determined by GC:

gas component	H_2	CO	CH_4	CO_2
obsd fraction	0.246	0.360	0.026	0.368

The chromatograms gave no indication of gases other than the four shown, which is in agreement with thermodynamic predictions. Standard deviations in the analyses were about 1% of the reported values.

Computer-generated equilibrium compositions are shown below for three equilibrium temperatures 600, 650, and 700 °C:

equilib temp	H_2	CO	CH_4	CO_2
600	0.198	0.236	0.015	0.551
650	0.212	0.373	0.010	0.405
700	0.215	0.519	0.006	0.260

The fractions for 650 °C agree reasonably well with the experimental data. Fractions for 600 and 700 °C are markedly different, which illustrates the sensitivity of the results to the assumed temperature. There are large changes in CO and CO_2 , which suggests that the CO/ CO_2 ratio is a good measure of equilibrium temperature.

The observed amount of methane is over twice what is predicted thermodynamically. This may indicate that methane forming reactions continue to occur as the gas passes through the lower temperature region of the reactor. Methane formation is favorable at lower temperature; for example, the equilibrium fraction of methane is 0.026 at 525 °C, and the maximum equilibrium methane concentration is 0.041 at about 350 °C.

The amounts of char product and condensed water recovered are also predicted in the calculations; however, neither quantity can be readily determined experimentally. This is because a layer of clean char is placed in the bottom of the reactor to avoid volatilization of organics during startup. Qualitatively, we observe a slight loss of char, about 10%, and roughly the same amount of water is recovered as we added initially. These observations are consistent with the thermodynamic predictions.

Gasification of Char with an Enhanced Reductive Zone. The previous results indicate that the equilibrium gas temperature is about 650 °C. Since equilibrium presumably occurs in the reductive zone, it should be possible to change the composition of the gas product by varying the temperature of the reductive zone. Increasing the temperature will lower the heat loss, promote endothermic chemistry, and increase the high-temperature residence time of the gas. The net effect should be to shift the equilibrium toward more CO and H_2 , thereby increasing the Btu value of the dry gas. This was investigated by conducting two gasifications of char with 10% water, in which the region surrounding the reductive zone was maintained first at 500 °C and second at 700 °C. These temperatures bracketed the estimated equilibrium temperature of 650 °C. Temperature control was accomplished by inserting the reactor in a tube furnace. The

experimental dry gas compositions, as determined by GC, are

reductive zone temp, °C	H ₂	CO	CH ₄	CO ₂
500	0.209	0.341	0.017	0.434
700	0.252	0.576	0.015	0.158

The calculated mole fractions in dry gas corresponding to the observed data are

equilib temp, °C	H ₂	CO	CH ₄	CO ₂
640	0.210	0.344	0.011	0.435
740	0.213	0.618	0.004	0.165

As observed in the previous experiment, the chromatogram indicated that only the four gases shown were present. There is excellent agreement between the 500 °C reductive zone results and the calculated results assuming a 640 °C equilibrium. The observed results are similar to those obtained previously without external heating of the zone. The 700 °C reductive zone results are quite different, and they correlate fairly well with calculated fractions at equilibrium temperatures of 740 °C. This demonstrates that the reductive zone processes are enhanced in this case. As previously observed, the dramatic change in the ratio of CO/CO₂ is predicted and the hydrogen predictions are reasonably accurate. However, as in the previous case, the amount of methane predicted is below that observed and the predicted decrease in methane with increasing temperature is also not observed. The calculated Btu/(standard ft³) values for the observed gas compositions are 189 (500 °C) and 323 (700 °C).

Calculated heat balance terms in the reductive zone experiments were found to be

reductive zone temp, °C	$\Delta_{\text{ex}}H$, kJ	$\Delta_{\text{g}}H(25\text{ }^\circ\text{C})$, kJ	fractional heat loss
500	-12.86	-26.26	0.490
700	-1.49	-17.54	0.085

The values expressed are per mole of char gasified. The fractional heat loss in the last column is the ratio $\Delta_{\text{ex}}H/\Delta_{\text{g}}H$ (25 °C), which indicates that there is very little heat loss when the reductive zone surroundings are held at 700 °C. The calculation showed that the adiabatic temperature for gasification of char containing 10% water is about 755 °C, which is very close to the equilibrium temperature of 740 °C. With a 500 °C reductive zone, the equilibrium temperature is estimated to be 640 °C, well below the adiabatic temperature, so that a substantial heat loss is obtained.

Gasification of a Char Containing Water and Hydrocarbons. The ultimate objective of these gasifications is to destroy complex waste mixtures containing organics. Thus, as a next step, it was decided to study a mixture of equal weights of decane, hexadecane, and octacosane, straight chain hydrocarbons of varying length. Gasification of this mixture will enable several factors to be determined. First, to what extent can gasification conditions be optimized so that only the synthesis gas components leave the reactor, in which case, the condensate will contain only water? Second, with nonoptimized oxygen flow rate, do these specific compounds tend to escape the reactor intact or do they tend to be converted to other substances. To study these questions, we will focus on analysis of the condensate.

A char containing 12.5%:12.5% mixture/water based on char weight was studied, and optimum results were obtained with an oxygen flow of 4.8 L/min. The gas burned with a blue flame, which indicates that there is little hydrocarbon content.

A hydrocarbon-rich gas burns with a yellow flame. GC/MS analysis showed only trace amounts of oil in the condensate, 1.9 ppm 1,3-dimethylbenzene, 8.3 ppm phenol, 17.5 ppm hexadecane, and 1.5 ppm phenanthrene. Thus, the thermodynamic predictions for the condensate are realized to within about 30 ppm of nonsynthesis gas components.

Gasification with 3.5 L/min (nonoptimized) oxygen flow gave poor results, as evidenced by the yellow burning gas. GC/MS analysis of the condensate showed large amounts of starting hydrocarbons (650 ppm decane and 560 ppm hexadecane) as well as small amounts of substituted phenols, naphthalenes, and other hydrocarbons, which indicates that the shorter hydrocarbons tend to escape the reactor intact.

Gasification of a Complex Refractory Waste. Used motor oil is a complex mixture that typically contains a fraction of sludge, and this was chosen for study as being representative of a real world waste. Complete characterization is economically unfeasible, and its refractory nature makes it difficult to destroy cleanly. While gasification of motor oil is feasible, the results of our studies show that it must be done with care. The first problem that may be encountered is formation of an aerosol in the effluent gas, which was particularly evident when gasification was done in a 1 in. diameter Vycor reactor. The char contained 25%:25% oil/water based on weight of char, and the oxygen flow was 3.5 L/min. Under these conditions, an aerosol is clearly visible in the gas product stream. The aerosol readily passes through the condenser and also through a granular char filter placed after the condenser. Some of the gas product was collected for analysis, and the remainder was flared as it emerged from the condenser through a tube. Under the conditions used, the flared gas exhibits a blue flame when the higher hydrocarbon content is low, and as the hydrocarbon content increases, the flame becomes increasingly yellow. An oil layer in the aqueous condensate is also observed in the latter case. With more sophisticated flare design, it is possible to produce a blue flame for most gas product compositions; however, in the present studies, the blue flame was used as a simple diagnostic test to determine proper operating parameters for each gasification.

With the Vycor reactor, about 15% of the condensate was an oil layer and the aqueous layer contained an estimated 1450 ppm dissolved organics, a combination of substituted benzenes, naphthalenes, straight chain hydrocarbons, and phenols. The presence of an aerosol during gasification is highly undesirable since it can facilitate the release of hazardous byproducts. The aerosol formation indicates inefficient gasification, both in the breakdown of larger organics in the ITZ and in their conversion to synthesis gas in the reductive zone. It was determined that by use of a larger diameter stainless steel reactor, the aerosol can be eliminated, and we attribute this to reduced heat loss.

A second requirement for efficient gasification of motor oil is sufficient water content in the char bed. A char sample with 25%:0% oil/water based on char weight was gasified with an oxygen flow of 4.8 L/min. The ITZ was difficult to sustain and had to be reinitiated several times. The flared gas product exhibited a yellow flame, and there was a 10% oil layer in the condensate. Gasification of a sample with 25%:12.5% oil/water at an oxygen flow of 2.5 L/min gave a sustainable ITZ but similar flame and condensate results. After having conducted numerous gasifications, we conclude that, as a rule of thumb, equal amounts of oil and water can be satisfactorily gasified. However, the oxidant flow rate is also important. This is illustrated with representative results for gasification of 12.5%:12.5% motor oil/water on char

obtained using a 1.25 in. stainless steel reactor:

	sample 1	sample 2	sample 3
oxygen flow, L/min	4.8	2.1	3.5
gas flame color	blue	blue/yellow	blue/yellow
condensate weight, g	8.0	7.1	8.7
oil layer fraction, %	trace	2	3
aq organics, ppm	<0.1	300	156

The results obtained for 4.8 L/min oxygen flow were near optimum. The flared gas exhibited a blue flame, and no oil was visible in the condensate. The organic content as determined by GC/MS was very low. The only substance found was phenol. Proton NMR showed very weak peaks consistent with phenol. Gasification at other oxygen flow rates produced blue/yellow gas flares, oil layers in the condensate, and greater aqueous organics. The compounds identified by GC/MS were benzenes, naphthalenes, anthracenes, straight chain hydrocarbons, and phenols.

Gasification of samples containing 25%:25% oil/water gave similar results:

	sample 4	sample 5	sample 6
oxygen flow, L/min	3.5	4.1	4.8
gas flame	blue/sl. yellow	blue/yellow	blue/yellow
condensate weight, g	11.3	10.7	14.9
oil layer fraction, %	trace	10	2
aq organics, ppm	124	300	414

The optimum oxygen flow rate is near 3.5 L/min. Thus, in the composition range of these samples, the oxygen flow rate seems to depend inversely on oil loading. The compounds found by GC/MS in sample 4 were mostly substituted phenols with smaller amounts of naphthalenes and benzenes. NMR results were consistent with phenol. Many compounds were found by GC/MS for samples 5 and 6. NMR spectra showed large peaks attributable to methyl and methylene groups, with only very small peaks downfield.

Gasification with a Continuous Feed Reactor. Another factor in the destruction of motor oil is the anticipated increase in throughput with use of continuous processing with the type reactor shown schematically in Figure 1. The gasification of motor oil was studied with such a reactor, and its use afforded the opportunity to study some additional factors of interest. First, the apparatus required for continuous mode operation is more complex. The rates at which char is fed into and removed from the reactor as well as the rate of oxidant flow must be carefully controlled so that the ITZ remains stationary. This control is facilitated by monitoring temperature at several points in the reactor. Considerable time was spent trouble shooting the apparatus. However with a smoothly operating continuous mode unit, much more material could be treated with each run and it was possible to extend the time for each run to as long as 90 min. This length of time gave the opportunity for operating parameters to be varied and optimized.

It was found that a relatively low loading of oil on the char was required for prolonged smooth operation, e.g., a mixture containing 5%:10% oil/water based on char. The rate of oxidant flow was varied, and the composition of the dry gas was monitored by GC at the different flow rates as shown in Table 1. There is larger experimental error for these data which may be attributable to the mode of operation or to the sampling procedure per se. However, the synthesis gas compositions generally agree with thermodynamic predictions. The presence of several percent of nonsynthesis gas

TABLE 1. Composition of Gas Obtained with Continuous Feed Reactor

	composition for given oxidant flow, %		
	7.9 L/min	8.7 L/min	10.5 L/min
hydrogen	15.42	21.93	17.89
propane	0.41	0.29	0.22
propylene	1.13	0.77	0.46
isobutane	0.00	0.00	0.00
<i>n</i> -butane	0.00	0.00	0.00
isopentane	0.16	0.09	0.08
<i>n</i> -pentane	0.00	0.00	0.00
carbon dioxide	49.81	35.06	35.24
ethylene	2.98	1.30	2.20
ethane	0.12	0.08	0.08
oxygen	0.46	0.19	0.42
nitrogen	0.81	0.45	0.87
methane	1.52	2.60	1.90
carbon monoxide	27.23	37.14	40.85

components, the majority being ethylene, propylene, and propane, is indicative of nonequilibrium conditions. The presence of oxygen and nitrogen is most likely caused by leaks. There is also a marked shift in the CO/CO₂ ratio with increased oxygen flow rate, which indicates a shift to higher temperature equilibrium.

The agreement between thermodynamic predictions and observed gas-phase composition obtained with optimized operating parameters indicates the absence of kinetic limitations in the formation of gas products. This is also consistent with the observed low organic content in the aqueous condensate.

Literature Cited

- (1) Cady, C.; Kapila, S.; Manahan, S. E.; Larsen, D. W.; Yanders, A. F. *Chemosphere* **1990**, *20*, 1959.
- (2) Larsen, D. W.; Manahan, S. E. U.S. Patent 4,978,477, 1990.
- (3) McGowin, A. E.; Kinner, L. L.; Manahan, S. E.; Larsen, D. W. *Chemosphere* **1991**, *22*, 1191.
- (4) Larsen, D. W.; Manahan, S. E. U.S. Patent 5,124,292, 1992.
- (5) McGowin, A. E.; Kinner, L. L.; Manahan, S. E.; Larsen, D. W. *Chemosphere* **1992**, *24*, 1867.
- (6) Kinner, L. L.; McGowin, A. E.; Manahan, S. E.; Larsen, D. W. *Environ. Sci. Technol.* **1993**, *27*, 482.
- (7) Kinner, L. L.; Manahan, S. E.; Larsen, D. W. *J. Environ. Sci. Health* **1993**, *A28*, 697.
- (8) Kinner, L. L.; McGowin, A. E.; Manahan, S. E.; Larsen, D. W. *Toxicol. Environ. Chem.* **1993**, *37*, 1.
- (9) McGowin, A. E.; Brendt, W.; Manahan, S. E.; Larsen, D. W. *Chemosphere* **1993**, *27*, 807.
- (10) McGowin, A. E.; Cady, C.; Manahan, S. E.; Larsen, D. W. *Chemosphere* **1993**, *27*, 779.
- (11) Medcalf, B. D.; Larsen, D. W.; Manahan, S. E. *Environ. Sci. Technol.* **1997**, *31*, 194.
- (12) Morlando, R. A.; Larsen, D. W.; Manahan, S. E. *Environ. Sci. Technol.* **1997**, *31*, 409.
- (13) Berry, V. J.; Parrish, D. R. *Petrol. Trans., AIME* **1960**, *219*, 124.
- (14) The commercially available program HSC Chemistry was developed by Outokompu Research Oy, Pori, Finland.
- (15) A typical analysis of char is 94.2% C, 5.5% H, and 0.3% O.
- (16) "HSC Chemisry" contains thermodynamic data for almost 10 000 compounds, including temperature dependent heat capacity data. It is also possible to correct for nonideality of gases; this was not done in the present case since these corrections are expected to be small given the gasification conditions, 1 bar and temperatures greater than 500 °C.
- (17) The mathematical basis for the calculation is given in e.g.: Kyle, B. G. *Chemical and Process Thermodynamics*; Prentice Hall: Englewood Cliffs, NJ, 1992; pp 431–436.
- (18) Medcalf, B. D.; Manahan, S. E.; Larsen, D. W. *Waste Manage.* **1998**, *197*, 18.
- (19) *Handbook of Chemistry and Physics*; Chemical Rubber Publishing Co: Cleveland, OH, 1955; pp 1770–1772, 37.
- (20) Noggle, J. W. *Physical Chemistry*; Harper Collins: 1996; pp 281–286.

(21) The adiabatic process temperature is found by an iterative procedure using HSC Chemistry. The initial reactant composition (char, water, octane, and oxygen), initial temperature, and final (output) temperature are selected. With these data, the product composition (char and gases) is calculated using HSC. Next, initial and final temperatures and compositions are input back into HSC, and the heat balance is evaluated. When the

final temperature equals the adiabatic temperature, $\Delta H = 0$. Thus the adiabatic temperature can be found by iteration.

Received for review November 30, 1998. Revised manuscript received May 26, 1999. Accepted June 16, 1999.

ES9812352